Novel contribution of cell surface and intracellular M1-muscarinic acetylcholine receptors to synaptic plasticity in hippocampus

ARTICLE *in* JOURNAL OF NEUROCHEMISTRY · MAY 2013

Impact Factor: 4.28 · DOI: 10.1111/jnc.12306 · Source: PubMed

12 AUTHORS, INCLUDING:

Abu Syed Md Anisuzzaman
Emory University
90 PUBLICATIONS **313** CITATIONS
SEE PROFILE

Takayoshi Masuoka
Kanazawa Medical University
26 PUBLICATIONS **289** CITATIONS
SEE PROFILE

Life Sciences 93 (2013) 17–23

Contents lists available at SciVerse ScienceDirect

Life Sciences

journal homepage: www.elsevier.com/locate/lifescie

Comparison of subcellular distribution and functions between exogenous and endogenous M1 muscarinic acetylcholine receptors

Shigeru Morishima [a,1], Abu Syed Md Anisuzzaman [a,1], Junsuke Uwada [a,b,1], Hatsumi Yoshiki [a], Ikunobu Muramatsu [a,b,c,*]

[a] Division of Pharmacology, Department of Biochemistry and Bioinformative Sciences, School of Medicine, University of Fukui, Eiheiji, Fukui 910-1193, Japan
[b] Organization for Life Science Advancement Programs, Graduate School of Medicine, University of Fukui, Eiheiji, Fukui 910-1193, Japan
[c] Child Development Research Center, Graduate School of Medicine, University of Fukui, Eiheiji, Fukui 910-1193, Japan

ARTICLE INFO

Article history:
Received 8 January 2013
Accepted 13 May 2013

Keywords:
Muscarinic acetylcholine receptor
M1 subtype
Intracellular GPCR
Endogenous and exogenous receptors
Ca^{2+} mobilization
ERK1/2 phosphorylation
Thymidine incorporation

ABSTRACT

Aims: Recombinant systems have been used for evaluating the properties of G-protein-coupled receptors (GPCRs) on the assumption of cell surface expression. However, many GPCRs, including muscarinic acetylcholine receptors (mAChRs), have also been reported to be distributed in intracellular organelles in native tissues and cell lines. In this study, we compared the pharmacological profiles of exogenously and endogenously expressed M1-mAChRs, and evaluated the functional properties of these receptors.
Main methods: Recombinant M1-mAChRs were expressed exogenously in Chinese hamster ovary cells (CHO-M1 cells) and compared with endogenously expressed M1-mAChRs in N1E-115 neuroblastoma cells. The pharmacological and functional profiles were evaluated using cell-permeable antagonists (1-quinuclidinyl-benzilate (QNB), pirenzepine and atropine) and cell-impermeable antagonists (N-methylscopolamine (NMS) or MT-7).
Key findings: M1-mAChRs were seen at the cell surface and intracellular sites in both cell lines. Under whole cell conditions, intracellular M1-mAChRs were mainly recognized by cell-permeable ligands, but scarcely by cell-impermeable ligands (at less than 100 nM). In CHO-M1 cells, M1-mAChR activation by carbachol resulted in Ca^{2+} mobilization, ERK1/2 phosphorylation and a reduction in thymidine incorporation, all of which were completely inhibited by MT-7, indicating the involvement of surface M1-mAChRs. In N1E-115 cells, Ca^{2+} mobilization occurred through surface M1-mAChRs, whereas ERK1/2 phosphorylation and acceleration of thymidine incorporation were mediated through intracellular M1-mAChRs.
Significance: Exogenous and endogenous M1-mAChRs are present at both the cell surface and the intracellular organelles, and the pharmacological properties of geographically distinct M1-mAChRs are different, and may depend on cell background and/or exogenous or endogenous origin.

Introduction

Recombinant receptors expressed in cultured cells represent a powerful tool to characterize receptor properties and have been widely used for drug development. However, it has recently been demonstrated that receptor properties are greatly influenced by cell background in which the receptor is expressed (Baker and Hill, 2007; Kenakin, 2003; Kenakin et al., 1995; Muramatsu et al., 2008; Nelson and Challiss, 2007). Muscarinic acetylcholine receptors (mAChRs) are one of the most familiar and important G-protein-coupled receptors (GPCRs), and are involved in many physiological functions, such as learning and memory in the central nervous system, and gland secretion or smooth muscle contraction in peripheral tissues (Brown, 2010; Eglen et al., 2001; Ehlert et al., 1997; Wess et al., 2007). mAChRs are present on the plasma membrane, bind agonists and transfer the signals into cells via their specific signal transduction pathways. Such properties of mAChRs have been confirmed in recombinant systems where mAChRs are artificially expressed as foreign receptors in many types of cells. Among five mAChR subtypes (M1–M5), M1, M3 and M5 subtypes couple with $G_{q/11}$ protein, causing hydrolysis of membrane phospholipids by phospholipase C and Ca^{2+} mobilization (Brown, 2010; Caulfield and Birdsall, 1998; van Koppen and Kaiser, 2003; Wess et al., 2007).

However, in addition to the plasma membrane distribution, many GPCRs, including mAChRs, are also reported to be distributed in intracellular organelles (Boivin et al., 2008; Calebiro et al., 2010; Mackenzie et al., 2000; McGrath et al., 1999; Mrzljak et al., 1993; Uwada et al., 2011). Classically, these intracellular receptors have been considered to be functionally inactive and to be involved in the processes of synthesis, catabolism and trafficking. However, there is emerging evidence that intracellular receptors can also display unique functions in several

* Corresponding author at: Child Development Research Center, Graduate School of Medicine, University of Fukui, 23-3 Eiheiji, Fukui 910-1193, Japan. Tel.: +81 776 61 8326; fax: +81 776 61 8130.
E-mail address: muramatu@u-fukui.ac.jp (I. Muramatsu).
[1] Equal contribution.

0024-3205/$ – see front matter © 2013 Elsevier Inc. All rights reserved.
http://dx.doi.org/10.1016/j.lfs.2013.05.013

GPCRs (Boivin et al., 2008). For example, metabotropic glutamate receptor $mGluR_5$ occurs at perinuclear membrane and causes slower Ca^{2+} mobilization and extracellular signal-regulated kinase (ERK1/2) activation in rat striatal neurons (Jong et al., 2005, 2009). In N1E-115 neuroblastoma cells, we have recently demonstrated that M1-mAChRs exist on both the plasma membrane and in the endoplasmic reticulum/Golgi apparatus, and that they activate different signal cascades (Uwada et al., 2011).

The purposes of the present study are to confirm the subcellular distribution and to compare the functions between exogenous and endogenous M1-mAChRs. We used recombinant M1-mAChRs transfected in Chinese hamster ovary cells (CHO-M1 cells) as representative exogenous receptors (Dorje et al., 1991) and endogenous M1-mAChRs expressing in N1E-115 neuroblastoma cells as controls. The results showed both surface and intracellular distribution of M1-mAChRs in both cell lines. However, the pharmacological properties of geographically distinct M1-mAChRs are different between these two systems, and may depend on cell background and/or homogeneous or heterogeneous expression.

Materials and methods

Drugs

The following drugs were used in the present study: 1-[N-methyl-^{3}H] scopolamine methyl chloride ([^{3}H]NMS, specific activity, 3.00 TBq/mmol), 1-quinuclidinyl-[phenyl-4-^{3}H]-benzilate ([^{3}H]QNB, specific activity, 1.81 TBq/mmol), and [methyl-^{3}H] thymidine (specific activity, 2.92 TBq/mmol) (GE Healthcare, Buckinghamshire, UK); muscarinic toxin 7 (MT-7) and muscarinic toxin 3 (MT-3) (Peptide Institute, Osaka, Japan); BODIPY 558/568 pirenzepine (BODIPY-pirenzepine; Invitrogen, Carlsbad, CA), atropine sulfate and carbachol hydrochloride (Nacalai Tesque, Kyoto, Japan); and pirenzepine (Tocris, Ellisville, MO). YM-254890 was kindly provided by Dr. J. Takasaki (Astellas Pharmaceutical Co. Ltd., Ibaraki, Japan).

Cell culture

The Chinese hamster ovary cell line stably expressing M1 mAChR (CHO-M1) was a gift from Dr. J. Wess (National Institutes of Health, Bethesda, MD). The mouse neuroblastoma cell line N1E-115 was purchased from American Type Cell Culture (Manassas, VA). Both cell lines were cultured in Dulbecco's modified Eagle's medium (Wako, Tokyo, Japan) supplemented with 10% fetal bovine serum in a humidified incubator with 5% CO_2 gas and 95% air. Cells were seeded 1 day before the experiment and log-phase proliferated cells were provided.

Radioligand binding assays

Hydrophilic [^{3}H]NMS and hydrophobic [^{3}H]QNB were used to detect surface and total mAChRs (Bylund et al., 2004; Galper et al., 1982; Uwada et al., 2011). Whole-cell binding assays were performed using these radioligands in CHO-M1 and N1E-115 cells. Cells were harvested by gentle scraping without trypsin, and were then incubated in 1 ml of Krebs-HEPES buffer (NaCl, 140 mM; KCl, 5.4 mM; $MgCl_2$, 1.2 mM; $CaCl_2$, 2.0 mM; NaH_2PO_4, 0.3 mM; glucose, 11.1 mM; HEPES, 5.4 mM; Na-HEPES, 4.6 mM, pH 7.4) for 4 h at 4 °C. Binding assays were performed in duplicate and nonspecific binding was defined as the amount of radioligand bound in the presence of 1 μM atropine. [^{3}H]NMS and [^{3}H]QNB at concentrations ranging from 50 to 2000 pM were used in saturation binding experiments. Binding competition experiments were performed in the presence of 500 pM of [^{3}H]NMS and [^{3}H]QNB with the addition of increasing concentrations of unlabeled drugs. Reactions were terminated by rapid filtration with a cell harvester onto Whatman GF/C glass filters (Rickly Hydrological, Columbus, OH) presoaked in 0.3% polyethyleneimine for 30 min. Filters were then washed three times and dried before measurement of filter-bound radioactivity by liquid scintillation counting.

Confocal microscopic observations

CHO-M1 and N1E-115 cells on glass bottom dishes were incubated with 0.1 μM BODIPY pirenzepine (membrane-permeable fluorescence-labeled M1 antagonist) in the absence or presence of mAChR antagonists for 30–40 min, and were subjected to confocal microscopic observation (TCS SP II; Leica Microsystems, Wetzlar, Germany). Ten minutes before observation, Hoechst 33258 stain (final concentration, 0.1 mg/ml; Invitrogen) was added to dishes in order to stain nuclei and cells were washed with Krebs-HEPES buffer just before microscopic observation.

Measurement of intracellular Ca^{2+}

Intracellular Ca^{2+} measurement was performed as described previously (Suzuki et al., 2007; Uwada et al., 2011). Briefly, sub-confluent CHO-M1 and N1E-115 cells were loaded with 5 μM Fura-2 AM (Dojindo, Kumamoto, Japan) in growth medium for 25 min, washed and then resuspended in Ca^{2+} assay buffer (136.9 mM NaCl, 5.4 mM KCl, 1.0 mM $MgCl_2$, 1.5 mM $CaCl_2$, 10 mM glucose and 10 mM HEPES, pH 7.4) with 1% serum. Immediately before intracellular Ca^{2+} measurement, buffer was exchanged with serum-free buffer. Intracellular Ca^{2+} concentration was measured by Fura-2 ratiofluorometry using a CAF-110 fluorescence spectrophotometer (Jasco, Tokyo, Japan). During measurements, cells were continuously stirred and kept suspended at 37 °C.

Western blot detection of ERK1/2

CHO-M1 and N1E-115 cells were seeded onto 35-mm dishes. After 24 h, cells were washed with PBS and maintained in serum-free medium for a further 20 h. Cells were then treated with 10 μM carbachol in the absence or presence of muscarinic antagonists or inhibitors that had been added 15 min prior to the addition of carbachol. At timed intervals, cells were then harvested using SDS sample buffer containing a phosphatase inhibitor cocktail (Roche, Penzberg, Germany). Each sample was subjected to SDS polyacrylamide gel electrophoresis followed by transfer to nitrocellulose membranes (GE Healthcare, Piscataway, NJ). The same sample was probed with antibodies against anti-phospho-ERK1/2 and anti-ERK1/2 (Cell Signaling Technology, Beverly, MA). Anti-rabbit IgG HRP-conjugated secondary antibody (Sigma) was used to reveal immunocomplexes, and was detected with an HRP detection kit (GE Healthcare).

[^{3}H] thymidine incorporation assay

Two days before the experiment, CHO-M1 and N1E-115 cells were seeded onto 24-well plates at a density of 3000 cells/well in triplicate. On the day of experiments, cultures were moved to low serum medium (2% fetal bovine serum) for 4 h. Antagonists or inhibitors were added 1 h before treatment with carbachol. After cells were incubated with an agonist for 1 h, [^{3}H]thymidine at a final concentration of 1 μCi/ml was added. After an additional 2-h incubation in the absence or presence of carbachol, cells were washed three times with ice-cold PBS and then incubated with 10% trichloroacetic acid for 5 min at 4 °C twice to remove unincorporated precursors to DNA. Cells were solubilized by 0.5 ml of 0.3 M NaOH and cell lysates were immediately neutralized with 2 ml of 10% trichloroacetic acid. After incubation for 1 h at 4 °C, the resulting precipitates were filtered through Whatman GF/C filters, dried and counted with a scintillation counter (Li et al., 2001).

Data analysis

Binding data were analyzed by Prism software (Graph Pad Software, San Diego, CA) and Origin software (Origin Lab, Northampton, MA) as described previously (Anisuzzaman et al., 2011). For saturation binding studies, data were fit to a one-site saturation binding isotherm. For competition studies, a two-site model was adopted only when the residual sums of squares were significantly less ($p < 0.05$) for a two-site fit of the data than for a one-site fit on *F* test comparison. All of the data are expressed as means ± standard error of the mean. Statistical differences in data were evaluated by analysis of variance (ANOVA) followed by Bonferroni's post-hoc test, when necessary, and were considered to be significant at $p < 0.05$.

Results

Binding of [^{3}H]QNB and [^{3}H]NMS

Under whole cell conditions, the hydrophobic [^{3}H]QNB and the hydrophilic [^{3}H]NMS have been used to detect total versus cell surface mAChRs, respectively, based on their distinct cell-permeability (Galper et al., 1982; Uwada et al., 2011). Fig. 1 shows the representative saturation curves for the specific binding of two radioligands at concentrations ranging from 50 to 2000 pM in CHO-M1 and N1E-115 cells at 4 °C. All saturation curves fit well with a hyperbolic saturation curve, suggesting that each radioligand bound to a single set of sites in each cell line. However, the maximum binding capacity (B_{max}) determined by cell permeable [^{3}H]QNB was significantly higher than that determined by cell-impermeable [^{3}H]NMS (Table 1). In contrast to binding densities, there were no large differences in dissociation constant (pKd) for each radioligand between both cell lines. From these results, it was considered that a significant amount of muscarinic binding sites may be present at intracellular sites, even under simple culture conditions.

As comparable amounts of muscarinic binding sites were detected at surface and intracellular sites, pharmacological profiles at both sites were examined in competition experiments with various drugs. Fig. 2 shows the competition curves for three representative muscarinic antagonists under whole cell conditions. Atropine, a subtype-nonselective hydrophobic ligand, completely inhibited the binding of both radioligands in a monotonic competitive manner (Fig. 2, Table 2). Non-radioactive NMS also monotonically competed with the [^{3}H]NMS binding, whereas the competition was biphasic at [^{3}H]QNB binding sites. Thus, 30–40% of [^{3}H]QNB binding sites were estimated as low sensitivity sites for NMS (left panel of Fig. 2A, B). A membrane-impermeable peptide toxin MT-7 (specific M1-mAChR antagonist) also competed with [^{3}H]NMS binding in CHO-M1 cells (right panel of Fig. 2A), although approximately 20% of [^{3}H]NMS binding remained as a MT-7-insensitive component in N1E-115 cells (right panel of Fig. 2B). [^{3}H]QNB binding sites in both cell lines displayed partial competition with MT-7. Pirenzepine (M1/M4-mAChR antagonist) completely inhibited the binding of both radioligands in both cell lines in a monotonic manner (Table 2). A minor component of mAChRs in N1E-115 cells was sensitive to low concentrations of MT-3 (M4-mAChR antagonist) (Table 2). These results suggest that M1-mAChRs are present on the cell surface and intracellular sites, and that intracellular M1-mAChRs are scarcely accessible by low concentrations of hydrophilic ligands ([^{3}H]NMS, NMS and MT-7), although at high concentrations, NMS also recognized intracellular sites. In addition to M1-mAChRs, M4 subtype was identified in a minor proportion (approximately 10% of total mAChRs) on the plasma membrane of N1E-115 cells, as reported previously (Fraeyman et al., 1991; Olianas et al., 2000).

Table 1
Binding affinities and densities for [^{3}H]NMS and [^{3}H]QNB in CHO-M1 and NIE-115 cells.

	CHO-M1		N1E-115	
	[^{3}H]-NMS	[^{3}H]-QNB	[^{3}H]-NMS	[^{3}H]-QNB
Bmax	3300 ± 190	5580 ± 175*	55 ± 2	109 ± 5*
pK_d	9.63 ± 0.21	9.85 ± 0.13	9.73 ± 0.05	9.48 ± 0.08

Whole cell-saturation binding experiments were carried out at 4 °C.
Bmax: fmol mg^{-1} total protein.
Data represent means ± SEM. for 5–7 experiments.
* Significantly different from [^{3}H]NMS binding ($p < 0.05$).

Carbachol also completely inhibited the binding of [^{3}H]QNB and [^{3}H]NMS in both cell lines (Fig. 3). The competition curves for carbachol were biphasic at [^{3}H]QNB binding sites, but monotonic at [^{3}H]NMS binding sites. The potency of carbachol was slightly higher in N1E-115 cells than in CHO-M1 cells (Table 2).

Microscopic observations with BODIPY-pirenzepine

In order to confirm subcellular distribution of M1-mAChRs, we performed microscopic observations with BODIPY-pirenzepine, a fluorescent marker for M1/M4-mAChRs. Red fluorescence signals of BODIPY-pirenzepine were widely distributed in CHO-M1 and N1E-115 cells (Fig. 4A, D), and small spots were particularly observed in cytoplasm and around the nucleus. In the presence of 0.1 μM MT-7, the fluorescence at marginal areas of the cell surface became less clear, but intracellular spots were still observed (Fig. 4B, E). Treatment with 10 μM atropine abolished all fluorescent signals (Fig. 4C, F).

Functional responses of surface and intracellular M1-mAChRs

As M1-mAChRs are distributed on the cell surface and intracellular sites in both CHO-M1 and N1E-115 cell lines, their possible functions were examined.

Ca^{2+} response

In both CHO-M1 and N1E-115 cells, carbachol transiently increased intracellular Ca^{2+}. Fig. 5A shows representative Ca^{2+} responses induced

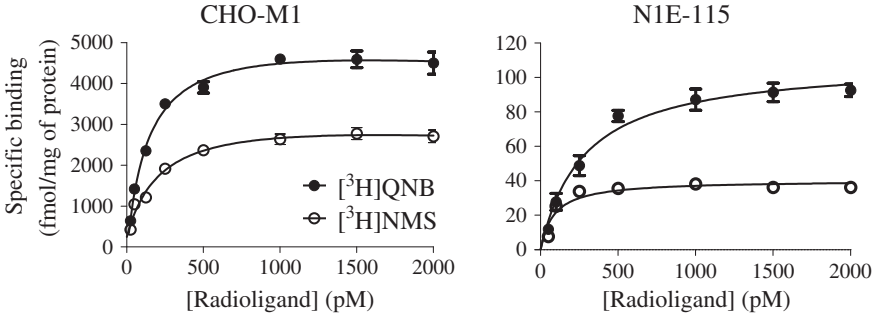

Fig. 1. Saturation curves for specific binding of [^{3}H]NMS and [^{3}H]QNB in CHO-M1 and N1E-115 cells. Whole cell binding was applied to CHO-M1 cells and N1E-115 cells at 4 °C. Data are representative of 5–7 experiments.

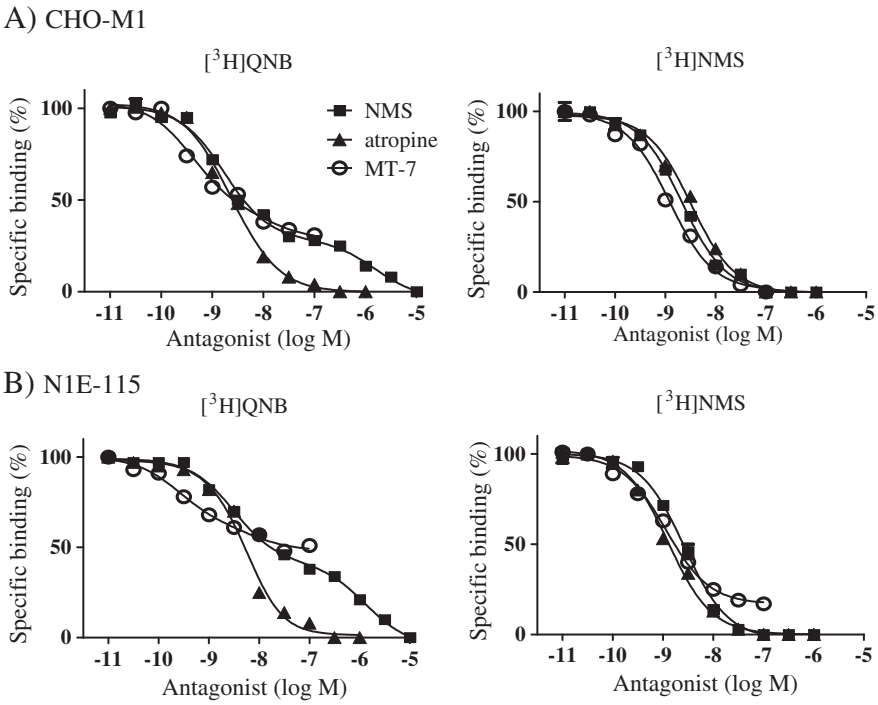

Fig. 2. Competition curves for MT-7, atropine and NMS at [^{3}H]NMS and [^{3}H]QNB binding sites in the CHO-M1 (A) and N1E-115 (B) cells. Whole cell binding experiments were conducted. Specific binding in the absence of antagonist was taken as 100%. Closed squares: NMS; closed triangles: atropine; open circles: MT-7. Data are representative of 4–5 experiments.

by 10 μM carbachol in CHO-M1 cells, where intracellular Ca^{2+} reached a peak at 10 s after application of carbachol, and then decreased. Net increases in Ca^{2+} were very different between both cell lines (Fig. 5B; approximately 1000 nM in CHO-M1 cells but 40 nM in N1E-115 cells); this was considered to be related to different densities of mAChRs between both cell lines (Table 1). Next, we examined the effects of two M1-antagonists (cell-impermeable MT-7 and cell-permeable pirenzepine). MT-7 (0.1 μM) and pirenzepine (10 μM) markedly inhibited or abolished the Ca^{2+} responses in the both cell lines (Fig. 5B). These results suggest that Ca^{2+} mobilization induced by carbachol in both cell lines is mediated through cell surface M1-mAChRs.

Table 2
Binding affinities for various ligands at [^{3}H]NMS and [^{3}H]QNB binding sites in CHO-M1 and NIE-115 cells.

	[^{3}H]NMS		[^{3}H]QNB	
	pKi high	pKi low	pKi high	pKi low
A. CHO-M1 cells				
Atropine	9.2 ± 0.2 (100%)		9.3 ± 0.1 (100%)	
NMS	9.9 ± 0.2 (100%)		10.1 ± 0.2 (72%)	7.1 ± 0.3 (28%)
Pirenzepine	8.3 ± 0.3 (100%)		8.2 ± 0.2 (100%)	
MT-7	9.8 ± 0.3 (100%)		9.7 ± 0.2 (68%)	– (32%)
MT-3		– (100%)		– (100%)
Carbachol	3.9 ± 0.2 (100%)		4.4 ± 0.2 (56%)	2.9 ± 0.2 (42%)
B. N1E-115 cells				
Atropine	9.2 ± 0.2 (100%)		9.4 ± 0.2 (100%)	
NMS	10.1 ± 0.1 (100%)		9.8 ± 0.1 (60%)	6.4 ± 0.2 (40%)
Pirenzepine	8.3 ± 0.3 (100%)		8.4 ± 0.3 (100%)	
MT-7	10.1 ± 0.1 (80%)	– (20%)	9.6 ± 0.2 (50%)	– (40%)
MT-3	9.6 ± 0.4 (20%)	– (80%)	9.4 ± 0.4 (10%)	– (90%)
Carbachol	5.3 ± 0.2 (100%)		5.9 ± 0.3 (63%)	3.5 ± 0.2 (37%)

Competition experiments with whole cells were carried out at 4 °C.
–: insensitive to 0.1 μM MT-7 or MT-3.
(%): proportion of each affinity site.
Data represent means ± S.E.M. for 4–5 experiments.

ERK1/2 activation

In both CHO-M1 and N1E-115 cell lines, carbachol produced ERK1/2 phosphorylation in a time-dependent manner. Fig. 6A shows the time course in CHO-M1 cells. Maximum activation was produced at 5–10 min after application of 10 μM carbachol. Phosphorylation was completely inhibited by MT-7 (0.1 μM) and pirenzepine (10 μM) in CHO-M1 cells (Fig. 6A), whereas phosphorylation in N1E-115 cells was resistant to MT-7 (Fig. 6B, right panel). Similar to pirenzepine, atropine abolished ERK1/2 activation in both cell lines (data not shown). These results suggested that carbachol-induced ERK1/2 phosphorylation was selectively produced through surface M1 mAChRs in CHO-M1 cells, while intracellular M1-mAChRs were exclusively involved in ERK1/2 phosphorylation in N1E-115 cells. ERK1/2 phosphorylation in CHO-M1 cells but not in N1E-115 cells (Fig. 6B) was inhibited by YM-254890 (1 μM).

[^{3}H]thymidine incorporation

Finally, we examined the effects of M1-mAChRs on cell growth in experiments with [^{3}H]thymidine. In CHO-M1 cells, uptake of [^{3}H]thymidine was significantly inhibited by 10 μM carbachol and the effects were antagonized by MT-7 (0.1 μM), pirenzepine (1 μM) or atropine (1 μM) (Fig. 7A). In contrast, [^{3}H]-thymidine incorporation was accelerated by carbachol in N1E-115 cells. This acceleration was not sensitive to MT-7, but was inhibited by pirenzepine and atropine (Fig. 7B). MT-3 (M4-mAChR antagonist) did not affect the carbachol-induced incorporation in N1E-115 cells (data not shown).

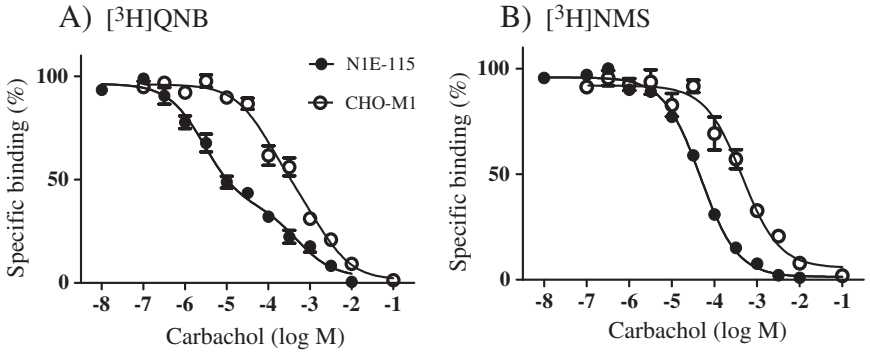

Fig. 3. Competition curves for carbachol at [^{3}H]QNB (A) and [^{3}H]NMS (B) binding sites in the CHO-M1 and N1E-115 cells. Open circles: CHO-M1 cells; closed circles: N1E-115 cells. Whole cell binding experiments were conducted at 4 °C. Data obtained from 4 experiments are summarized.

Discussion

mAChRs have been considered to be representative plasma membrane receptors. However, the present study using CHO-M1 and N1E-115 cells revealed that M1-mAChRs are distributed on the plasma membrane and at intracellular sites, irrespective of exogenous or endogenous origin. This was demonstrated by: 1) different binding densities of hydrophobic [^{3}H]QNB and hydrophilic [^{3}H]NMS; 2) different accessibilities of cell-permeable and -impermeable ligands; and 3) microscopic observation of BODIPY-pirenzepine-binding sites. As comparable amounts of M1-mAChRs were detected at both surface and intracellular sites under conditions where cells were simply cultured and not stimulated, it is likely that M1-mAChRs are constitutively expressed at both plasma membrane and intracellular sites.

Recently, intracellular distribution and functions have been demonstrated in several GPCRs (Boivin et al., 2008; Calebiro et al., 2010). Therefore, possible functions of geographically distinct M1-mAChRs were examined in CHO-M1 cells and N1E-115 cells. Regardless of heterogeneous and homogeneous receptors, activation of M1-mAChRs by carbachol increased intracellular Ca^{2+}, and this response was completely inhibited by a cell-impermeable M1-antagonist MT-7 and a $G_{q/11}$ inhibitor YM-254890 (Takasaki et al., 2004). Thus, it is likely

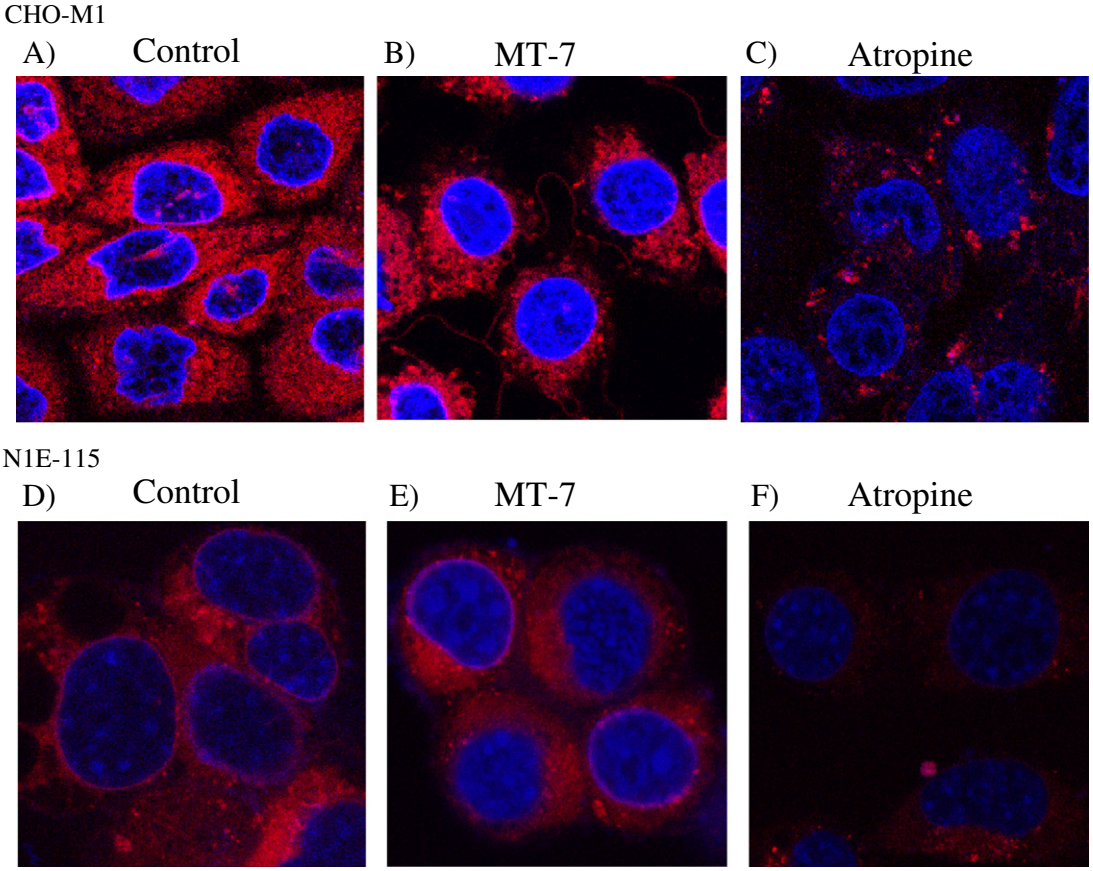

Fig. 4. Confocal microscopic images of CHO-M1 (A, B, C) and N1E-115 cells (D, E, F). Both cell lines were incubated with BODIPY-pirenzepine (red) and Hoechst 33258 (blue). Cells were coincubated with 0.1 μM MT-7 (middle panels) or 10 μM atropine (right panels).

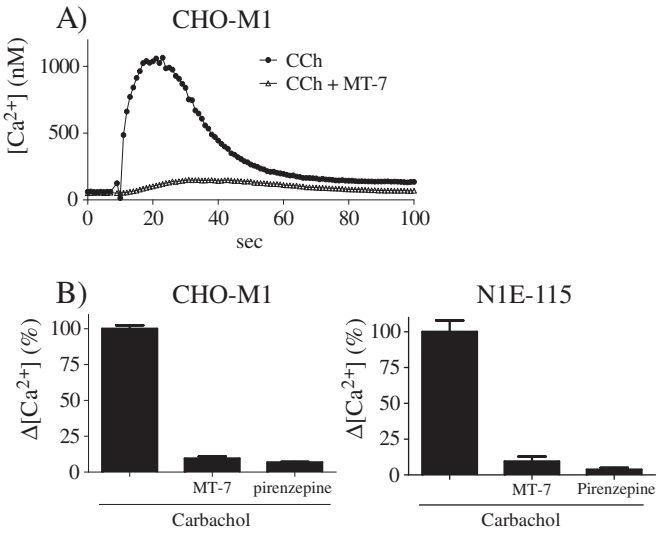

Fig. 5. Ca^{2+} responses to carbachol in CHO-M1 and N1E-115 cells. (A) Representative traces of Ca^{2+} transient response to carbachol (10 μM CCh) in the absence or presence of 0.1 μM MT-7 in CHO-M1 cells. (B) Effects of 0.1 μM MT-7 and 10 μM pirenzepine on Ca^{2+} transient response to CHO-M1 and N1E-115 cells. Ca^{2+} transient response was measured at peak. Mean ± S.E.M. of 3–4 experiments. *Significantly different from control (carbachol alone, $p < 0.01$).

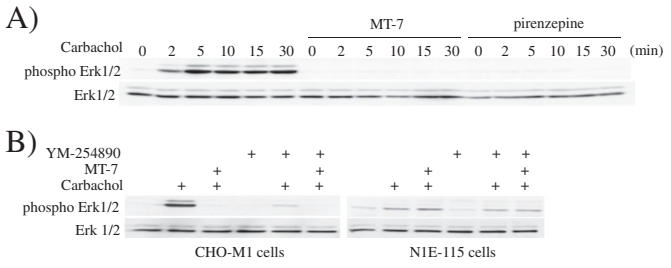

Fig. 6. ERK1/2 activation by carbachol. (A) Time course of ERK1/2 phosphorylation in the absence or presence of MT-7 and pirenzepine in CHO-M1 cells. MT-7 (0.1 μM) or pirenzepine (10 μM) was treated for 15 min before carbachol (10 μM) application. (B) Effects of MT-7 and YM254890 on carbachol-induced ERK1/2 phosphorylation in CHO-M1 cells and N1E-115 cells.

that the Ca^{2+} mobilization in CHO-M1 and N1E-115 cells was selectively mediated through surface M1-mAChRs in a $G_{q/11}$-protein-dependent manner.

In addition to Ca^{2+} mobilization, M1-mAChRs are known to activate MAP kinase (Hamilton and Nathanson, 2001; Rosenblum et al., 2000). In the present study, the ERK1/2 pathway was activated by carbachol in both cell lines. However, the ERK1/2 phosphorylation in CHO-M1 cells was completely inhibited by mAChR antagonists including cell-impermeable MT-7 and a $G_{q/11}$ inhibitor YM-254890, whereas the phosphorylation in N1E-115 cells was resistant to MT-7 and YM-254890. These results strongly suggest that surface and intracellular M1-AChRs in both cell lines have ligand binding properties but that the intracellular M1-mAChRs may be functionally inactive in CHO-M1 cells in contrast to N1E-115 cells at least under the present assay conditions.

Another interesting difference was observed in [^{3}H]thymidine incorporation. Carbachol inhibited [^{3}H]thymidine incorporation in CHO-M1 cells, but augmented the incorporation in N1E-115 cells, suggesting that cell growth is differently regulated by M1-mAChRs in both cell lines. The relationship between M1-mAChR and cell proliferation has been well studied, but the results remain controversial (Costa et al., 2001). Ashkenazi et al. reported an acceleration of [^{3}H]thymidine incorporation by mAChR in M1-transfected CHO cells and primary cultured rat brain astrocytes (Ashkenazi et al., 1989). Such a stimulatory effect on cell growth was also demonstrated in M1-mAChR-transfected NIH 3T3 cells and primary cultured cortical neurons (Stephens et al., 1993). On the other hand, inhibitory effects of transfected M1-mAChRs on cell growth have been reported in A9L and CHO cells (Baumgold and Dyer, 1994; Conklin et al., 1988). Interestingly, the present study shows that the reduction in [^{3}H]thymidine incorporation in CHO-M1 cells was completely inhibited by cell-impermeable MT-7, while the acceleration in N1E-115 cells was resistant to MT-7. Therefore, it is likely that variable effects of M1-mAChRs on cell proliferation may be in part related to differences in the subcellular localization of M1-mAChRs and/or in their subsequent signal cascades in each cell line (Costa et al., 2001).

Classically, intracellular M1-mAChRs have been considered to be a premature type, or a 'depot' of newly synthesized receptors destined to replenish the plasma membrane when needed, or internalized receptors after agonist stimulation. Indeed, under the present assay conditions, the surface M1-mAChRs only were functional in CHO-M1 cells, whereas the surface and intracellular M1-mAChRs were used in N1E-115 cells. How can intracellular M1-mAChRs work in N1E-115 cells but not work in CHO-M1 cells? This may be related to the different origins of M1-mAChRs and to the different cell lines; endogenous M1-mAChRs can couple with an inherent signal transduction pathway in N1E-115 cells, while such signaling pathway may be incomplete in CHO-M1 cells or the transfected receptors may not effectively couple to the signaling pathway. It is also interesting to note higher affinity

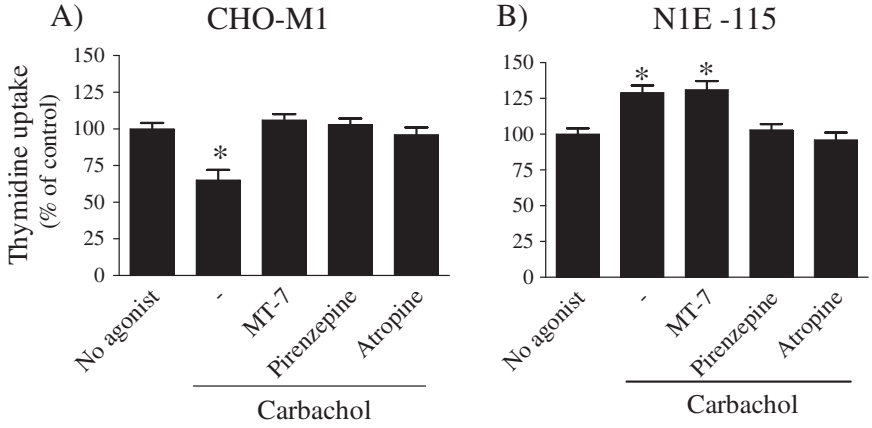

Fig. 7. Effects of carbachol on [^{3}H]-thymidine uptake in CHO-M1 cells (A) and N1E-115 cells (B). Cells were stimulated with 10 μM carbachol in the absence or presence of 0.1 μM MT-7, 1 μM pirenzepine or 1 μM atropine. Mean value in the absence of any drugs was taken as 100%. Mean ± S.E.M. of 4–5 experiments. *Significantly different from control (no agonist) ($p < 0.05$).

for carbachol of endogenous M1-mAChRs in N1E-115 cells than exogenous M1-mAChRs in CHO-M1 cells. Alternatively, the difference may reflect the distinct plasma membrane permeability of carbachol in the cell lines, although carbachol as well as hydrophilic NMS at high concentrations could have access to the binding sites of [^{3}H]QNB and [^{3}H]NMS. In general, carbachol and ACh possess a positively charged quaternary ammonium substituent, which might not permeate easily through the plasma membrane at low concentrations and for short exposure. However, as ACh and carbachol were previously reported to be taken up into mouse cerebral cortex slices (Liang and Quastel, 1969), it is possible that the putative transporter system is present and functional in N1E-115 neuroblastoma cells, but not in non-neuronal cells such as CHO cells. These points require further examination in future experiments.

Conclusion

The present study shows that M1-mAChRs are distributed on the plasma membrane and in intracellular organelles, even though their origin is exogenous or endogenous, and that their functional abilities may strongly depend on cell background, suggesting pharmacological polymorphism of M1-mAChRs. As subcellular distribution of M1-mAChRs has been demonstrated in the central nervous system in immunohistochemical studies (Mrzljak et al., 1993; Yamasaki et al., 2010), pharmacological diversity between surface and intracellular M1-mAChRs in native tissues may become an important clue in exploring cholinergic mechanisms in higher brain functions such as learning and memory (Brown, 2010; Wess et al., 2007).

Conflict of interest statement

The authors declare no conflicts of interest.

Acknowledgments

This work was supported in part by a Grant-in-Aid for Scientific Research from the Ministry of Education, Culture, Sports, Science and Technology of Japan, by a grant from the Smoking Research Foundation of Japan, and by Organization for Life Science Advancement Programs (Research and Education Program for Life Science, Translational Research Program) and Life Science Research Laboratory, University of Fukui.

References

Anisuzzaman ASM, Nishimune A, Yoshiki H, Uwada J, Muramatsu I. Influence of tissue integrity on pharmacological phenotypes of muscarinic acetylcholine receptors in the rat cerebral cortex. J Pharmacol Exp Ther 2011;339:186–93.
Ashkenazi A, Ramachandran J, Capon DJ. Acetylcholine analogue stimulates DNA synthesis in brain-derived cells via specific muscarinic receptor subtypes. Nature 1989;340:146–50.
Baker JG, Hill SJ. Multiple GPCR conformations and signalling pathways: implications for antagonist affinity estimates. Trends Pharmacol Sci 2007;28:374–81.
Baumgold J, Dyer K. Muscarinic receptor-mediated inhibition of mitogenesis via a protein kinase C-independent mechanism in M1-transfected A9 L cells. Cell Signal 1994;6:103–8.
Boivin B, Vaniotis G, Allen BG, Hebert TE. G protein-coupled receptors in and on the cell nucleus: a new signaling paradigm? J Recept Signal Transduct Res 2008;28:15–28.
Brown DA. Muscarinic acetylcholine receptors (mAChRs) in the nervous system: some functions and mechanisms. J Mol Neurosci 2010;41:340–6.
Bylund DB, Deupree JD, Toews ML. Radioligand-binding methods for membrane preparations and intact cells. Methods Mol Biol 2004;259:1–28.
Calebiro D, Nikolaev VO, Persani L, Lohse MJ. Signaling by internalized G-protein-coupled receptors. Trends Pharmacol Sci 2010;31:221–8.
Caulfield MP, Birdsall NJ. International Union of Pharmacology. XVII. Classification of muscarinic acetylcholine receptors. Pharmacol Rev 1998;50:279–90.
Conklin BR, Brann MR, Buckley NJ, Ma AL, Bonner TI, Axelrod J. Stimulation of arachidonic acid release and inhibition of mitogenesis by cloned genes for muscarinic receptor subtypes stably expressed in A9 L cells. Proc Natl Acad Sci U S A 1988;85:8698–702.
Costa LG, Guizzetti M, Oberdoerster J, Yagle K, Costa-Mallen P, Tita B, et al. Modulation of DNA synthesis by muscarinic cholinergic receptors. Growth Factors 2001;18:227–36.
Dorje F, Wess J, Lambrecht G, Tacke R, Mutschler E, Brann MR. Antagonist binding profiles of five cloned human muscarinic receptor subtypes. J Pharmacol Exp Ther 1991;256:727–33.
Eglen RM, Choppin A, Watson N. Therapeutic opportunities from muscarinic receptor research. Trends Pharmacol Sci 2001;22:409–14.
Ehlert FJ, Ostrom RS, Sawyer GW. Subtypes of the muscarinic receptor in smooth muscle. Life Sci 1997;61:1729–40.
Fraeyman NH, Buyse MA, Lefebvre RA. Study of the muscarinic receptor subtypes in N1E 115 mouse neuroblastoma cells. Pharmacol Res 1991;23:33–40.
Galper JB, Dziekan LC, O'Hara DS, Smith TW. The biphasic response of muscarinic cholinergic receptors in cultured heart cells to agonists. Effects on receptor number and affinity in intact cells and homogenates. J Biol Chem 1982;257:10344–56.
Hamilton SE, Nathanson NM. The M1 receptor is required for muscarinic activation of mitogen-activated protein (MAP) kinase in murine cerebral cortical neurons. J Biol Chem 2001;276:15850–3.
Jong YJ, Kumar V, Kingston AE, Romano C, O'Malley KL. Functional metabotropic glutamate receptors on nuclei from brain and primary cultured striatal neurons. Role of transporters in delivering ligand. J Biol Chem 2005;280:30469–80.
Jong YJ, Kumar V, O'Malley KL. Intracellular metabotropic glutamate receptor 5 (mGluR5) activates signaling cascades distinct from cell surface counterparts. J Biol Chem 2009;284:35827–38.
Kenakin T. Predicting therapeutic value in the lead optimization phase of drug discovery. Nat Rev Drug Discov 2003;2:429–38.
Kenakin T, Morgan P, Lutz M. On the importance of the "antagonist assumption" to how receptors express themselves. Biochem Pharmacol 1995;50:17–26.
Li BS, Ma W, Zhang L, Barker JL, Stenger DA, Pant HC. Activation of phosphatidylinositol-3 kinase (PI-3 K) and extracellular regulated kinases (Erk1/2) is involved in muscarinic receptor-mediated DNA synthesis in neural progenitor cells. J Neurosci 2001;21:1569–79.
Liang CC, Quastel JH. Uptake of acetylcholine in rat brain cortex slices. Biochem Pharmacol 1969;18:1169–85.
Mackenzie JF, Daly CJ, Pediani JD, McGrath JC. Quantitative imaging in live human cells reveals intracellular alpha(1)-adrenoceptor ligand-binding sites. J Pharmacol Exp Ther 2000;294:434–43.
McGrath JC, Mackenzie JF, Daly CJ. Pharmacological implications of cellular localization of alpha1-adrenoceptors in native smooth muscle cells. J Auton Pharmacol 1999;19:303–10.
Mrzljak L, Levey AI, Goldman-Rakic PS. Association of m1 and m2 muscarinic receptor proteins with asymmetric synapses in the primate cerebral cortex: morphological evidence for cholinergic modulation of excitatory neurotransmission. Proc Natl Acad Sci U S A 1993;90:5194–8.
Muramatsu I, Morishima S, Suzuki F, Yoshiki H, Anisuzzaman AS, Tanaka T, et al. Identification of alpha 1L-adrenoceptor in mice and its abolition by alpha 1A-adrenoceptor gene knockout. Br J Pharmacol 2008;155:1224–34.
Nelson CP, Challiss RA. "Phenotypic" pharmacology: the influence of cellular environment on G protein-coupled receptor antagonist and inverse agonist pharmacology. Biochem Pharmacol 2007;73:737–51.
Olianas MC, Maullu C, Adem A, Mulugeta E, Karlsson E, Onali P. Inhibition of acetylcholine muscarinic M(1) receptor function by the M(1)-selective ligand muscarinic toxin 7 (MT-7). Br J Pharmacol 2000;131:447–52.
Rosenblum K, Futter M, Jones M, Hulme EC, Bliss TV. ERKI/II regulation by the muscarinic acetylcholine receptors in neurons. J Neurosci 2000;20:977–85.
Stephens EV, Kalinec G, Brann MR, Gutkind JS. Transforming G protein-coupled receptors transduce potent mitogenic signals in NIH 3T3 cells independent on cAMP inhibition or conventional protein kinase C. Oncogene 1993;8:19–26.
Suzuki F, Morishima S, Tanaka T, Muramatsu I. Snapin, a new regulator of receptor signaling, augments alpha1A-adrenoceptor-operated calcium influx through TRPC6. J Biol Chem 2007;282:29563–73.
Takasaki J, Saito T, Taniguchi M, Kawasaki T, Moritani Y, Hayashi K, et al. A novel Galphaq/11-selective inhibitor. J Biol Chem 2004;279:47438–45.
Uwada J, Anisuzzaman AS, Nishimune A, Yoshiki H, Muramatsu I. Intracellular distribution of functional M(1)-muscarinic acetylcholine receptors in N1E-115 neuroblastoma cells. J Neurochem 2011;118:958–67.
van Koppen CJ, Kaiser B. Regulation of muscarinic acetylcholine receptor signaling. Pharmacol Ther 2003;98:197–220.
Wess J, Eglen RM, Gautam D. Muscarinic acetylcholine receptors: mutant mice provide new insights for drug development. Nat Rev Drug Discov 2007;6:721–33.
Yamasaki M, Matsui M, Watanabe M. Preferential localization of muscarinic M1 receptor on dendritic shaft and spine of cortical pyramidal cells and its anatomical evidence for volume transmission. J Neurosci 2010;30:4408–18.